29th International Conference
ENGINEERING MECHANICS 2023
Milovy, Czech Republic, May 9 – 11, 2023

CALIBRATED FINITE VOLUME METHOD-BASED SIMULATION FRAMEWORK FOR LASER SHOCK PEENING

Isoz M.*, Gruber P., Schmidt J.***, Kubíčková L.†, Štefan J.‡, Kaufman J.§, Brajer J.¶, Gabriel D.‖**

Abstract: *Modern and highly competitive industry seeks components with high strength and fatigue resistance. Both of these properties may be improved by peening of the component surface and the standard peening processes, such as the shot peening, are widely used in both automotive and aerospace industries. The laser shock peening (LSP), i.e. hardening of the material surface by a laser-induced shock wave, is a modern alternative to the standard peening. Concurrently, the industrial applications of LSP are promoted by recently emerged affordable high power-density lasers. However, the nascent LSP applications are still mostly a trial-and-error processes based on an extensive experimental testing. Consequently, we focused on a highly application-driven development of a framework for LSP modeling, and the internal workings and results of which are the focus of the present contribution.*

Keywords: laser shock peening, modeling, finite volume method, OpenFOAM.

1. Introduction

Attempts on laser-induced changes in properties of materials have been made since 1960s and 70s (Penner and Sharma, 1966; Fabbro et al., 1989). However, it was mostly during the last two decades that the availability of reasonably-priced powerful lasers made laser shock processing a competitive alternative to classical surface treatments for improving fatigue, corrosion and wear properties of metallic materials Hfaiedh et al. (2015). In the following, we will concentrate on the variant of the laser shock processing known as the laser shock peening, which we will abbreviate as LSP.

LSP have been studied using finite element analysis since the end of 1990s, see Braisted and Brockman (1999) and a number of subsequent publications. However, its simulation via other methods for numerical solution of partial differential equations, such as the finite difference or finite volume method is virtually non-existing. Still, especially the finite volume method (FVM) can provide interesting characteristics for simulating the shock-wave propagation, especially on non-perfect meshes, which are of interest for industrial applications.

In this contribution, we present an FVM-based simulation framework for LSP implemented in the open-source C++ library OpenFOAM (OpenCFD, 2007), which is based on the finite volume method. In particular, we roughly follow the approaches described by Cardiff et al. (2017). However, the resulting solvers are optimized specifically for application for laser shock peening. Furthermore, we apply a novel coupling between explicit and implicit integration of the system governing equation designed specifically for domain decomposition tailor-made for FVM-based LSP modeling.

* Ing. Martin Isoz, Ph.D.: Institute of Thermomechanics, Czech Academy of Sciences (CAS), Dolejškova 1402/5; 182 00, Prague; CZ, isozm@it.cas.cz
** Ing. Pavel Gruber, Ph.D.: Institute of Thermomechanics, CAS, Dolejškova 1402/5; 182 00, Prague; CZ
*** Ing. Jaroslav Schmidt: Institute of Thermomechanics, CAS, Dolejškova 1402/5; 182 00, Prague; CZ
† Bc. Lucie Kubíčková: Institute of Thermomechanics, CAS, Dolejškova 1402/5; 182 00, Prague; CZ
‡ Ing. Jan Štefan, Ph.D.: Institute of Thermomechanics, CAS, Dolejškova 1402/5; 182 00, Prague; CZ
§ Ing. Jan Kaufman, Ph.D.: HiLASE Centre, Institute of Physics, CAS, Za Radnicí 828; 252 41, Dolní Březany; CZ
¶ Ing. Jan Brajer, Ph.D.: HiLASE Centre, Institute of Physics, CAS, Za Radnicí 828; 252 41, Dolní Březany; CZ
‖ Ing. Dušan Gabriel, Ph.D.: Institute of Thermomechanics, CAS, Dolejškova 1402/5; 182 00, Prague; CZ

ISSN: 1805-8256, doi: 10.21495/em2023-103

The presented approach to LSP modeling is strongly application oriented. As such, it is supplemented by a specifically designed experiment allowing to calibrate the proposed model for a concrete laser-material combination and allowing for industrially-relevant large-scale simulations.

2. Simulation framework fundametals

Let us consider a specimen submitted to a LSP process. The specimen geometry is represented by a bounded open connected domain Ω with boundary $\Gamma = \partial\Omega$. Furthermore, irreversible phenomena caused by a propagation of laser-induced plastic shock waves are assumed to occur solely in $\Omega^{\mathrm{s}} \subset \Omega$ with boundary Γ^{s}.

During the LSP process, the specimen is exposed to a set of laser shots $\mathcal{L} = \{\ell_1, \ell_2, \ldots, \ell_N\}$ applied to the processed boundary $\Gamma^{\mathrm{s}}_{\mathrm{p}} \subset \Gamma^{\mathrm{s}}$. In particular, the i-th shot ℓ_i is represented by spatially and temporally varying pressure loading p_{ℓ_i} applied to $\Gamma^{\mathrm{s}}_{\mathrm{p},i} \subset \Gamma^{\mathrm{s}}_{\mathrm{p}}$. The duration of pressure loading for ℓ_i is in tens of nanoseconds while the individual shots are deposited with an interval of 0.1 s. This splitting of temporal scales allows for decomposition of the LSP simulation into a series of N consecutive steps.

Each step comprises a dynamic plastic wave propagation followed by a pseudo-static relaxation. Let $\boldsymbol{u}$ and $\boldsymbol{u}_{\mathrm{r}}$ mark displacements from the dynamic and relaxation sub-steps, respectively, and let ε_{p} be the plastic strain. Then, initial conditions and initial internal state at i-th simulation step are

$$\boldsymbol{u}^i = \boldsymbol{u}^{i-1}_{\mathrm{r}}, \quad \dot{\boldsymbol{u}}^i = \ddot{\boldsymbol{u}}^i = 0, \quad \varepsilon^i_{\mathrm{p}} = \varepsilon^{i-1}_{\mathrm{p}} \quad \text{in} \quad \Omega^{\mathrm{s}} \cap \Gamma^{\mathrm{s}}. \tag{1}$$

Both the dynamic and relaxation sub-steps are simulated under the small strains settings $\varepsilon = \frac{1}{2}\left(\nabla\boldsymbol{u} + \boldsymbol{u}\nabla\right)$ with damping effects and body forces neglected. The dynamic plastic wave propagation is described by the Cauchy momentum equation

$$\nabla \cdot \sigma^i = \rho\ddot{\boldsymbol{u}}^i \quad \text{on} \quad \Omega^{\mathrm{s}}, \quad \forall \ell_i \in \mathcal{L}\,, \tag{2}$$

where σ is the stress tensor and ρ the material density. The dynamic momentum balance is supplemented by boundary conditions

$$\boldsymbol{u}^i = \boldsymbol{0} \quad \text{on} \quad \Gamma^{\mathrm{s}}_{\mathrm{D}} := \Gamma^{\mathrm{s}} \cap \Gamma_{\mathrm{D}}, \quad \boldsymbol{n} \cdot \sigma^i = \begin{cases} \boldsymbol{n}\, p_{\ell_i} & \text{on} \quad \Gamma^{\mathrm{s}}_{\mathrm{p},i} \\ \boldsymbol{0} & \text{on} \quad \Gamma^{\mathrm{s}} \setminus \Gamma^{\mathrm{s}}_{\mathrm{D}} \setminus \Gamma^{\mathrm{s}}_{\mathrm{p},i} \end{cases}, \quad \forall \ell_i \in \mathcal{L} \tag{3}$$

where Γ_{D} and $\Gamma^{\mathrm{s}} \setminus \Gamma^{\mathrm{s}}_{\mathrm{D}} \setminus \Gamma^{\mathrm{s}}_{\mathrm{p},i}$ are the Dirichlet and Neumann parts of Γ, respectively. The system (2) with boundary conditions (3) is integrated explicitly using the central difference scheme. The material internal state is represented by $\varepsilon^i_{\mathrm{p}}$, which evolves under the von Mises yield criterion.

The relaxation step is simulated as a static linear elasticity problem with fixed internal state $\varepsilon^i_{\mathrm{p}}$. Thus,

$$\nabla \cdot \sigma^i_{\mathrm{r}} = \boldsymbol{0} \text{ in } \Omega, \quad \boldsymbol{u}^i_r = \boldsymbol{0} \text{ on } \Gamma_{\mathrm{D}}, \quad \boldsymbol{n} \cdot \sigma^i = \boldsymbol{0} \text{ on } \Gamma \setminus \Gamma_{\mathrm{D}}, \quad \forall \ell_i \in \mathcal{L}, \tag{4}$$

$$\varepsilon^i_0 = \begin{cases} \varepsilon^i_{\mathrm{p}} & \text{on} \quad \Omega^{\mathrm{s}} \cap \Gamma^{\mathrm{s}} \\ 0 & \text{on} \quad \Omega \setminus (\Omega^{\mathrm{s}} \cap \Gamma^{\mathrm{s}}) \end{cases}, \quad \forall \ell_i \in \mathcal{L}\,, \tag{5}$$

where we consider the Hooke's law with initial strains $\sigma = 2\mu\left(\varepsilon - \varepsilon_0\right) + \lambda \mathrm{tr}\left(\varepsilon - \varepsilon_0\right)\mathrm{I}$.

Computational remarks The domain Ω is discretized utilizing a cell-centered variant of the finite volume method. In numerous applications $\Omega^{\mathrm{s}} \ll \Omega$. Furthermore, the dynamic problem has stricter requirements on the mesh quality then the static relaxation. Consequently, it is advantageous to define the dynamic problem only on Ω^{s}, see (2). However, the need for an efficient parallelization of both the dynamic and relaxation sub-steps necessitates an independent domain decompositions of Ω^{s} and Ω. Data sharing between the two domain decomposition is supplied by a direct one-to-one map.

3. Framework calibration and validation

The goal of the present research is to provide a computationally efficient simulation tool able to predict "true" residual stresses for problems relevant to tool engineers. To fulfill the later, the simulation framework, which is based on the simplest phenomenological material model, is complemented by a specifically designed calibration experiment. In particular, we calibrate (i) the spatial and temporal evolution of the laser-induced pressure loading, and (ii) the von Mises material yield strength. The calibration goal is to fit measured residual stresses on the specimen surface.

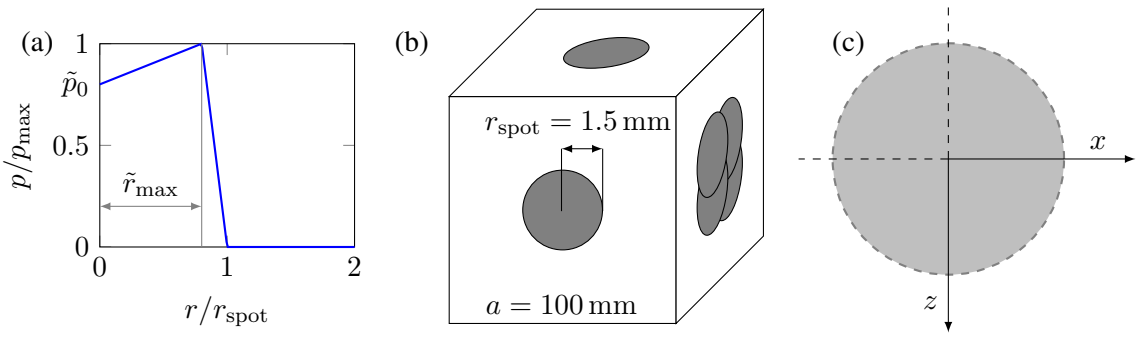

Fig. 1: (a) Spatial pressure intensity distribution. (b) Cube specimen with calibration single shots and validation quadruple shot in face-centers. (c) Sampling lines through a single shot.

Assumed pressure loading In time, the pressure pulse is assumed to be a simple tent function for which the total pulse duration (T_{t}) is the calibrated parameter. In space, the pressure pulse is assumed to be axi-symmetric and piecewise linear with maximum pressure intensity $p_{\max}$ achieved at $r_{\max}$ and the overall shape as indicated in Fig. 1a. The calibrated parameters are $\tilde{p}_0$, $p_{\max}$, and $\tilde{r}_{\max}$.

C	Mn	Si	P	S	Cr	Ni	Cu	Al
0.17	1.25	0.42	0.009	0.006	0.1	0.08	0.15	0.027

Tab. 1: Chemical composition of the used S355J2

Specimen The single-shot calibration experiment was designed in such a way that it corresponds as close as possible to a single circular LSP pulse applied to a half-space. For such a case, no wave reflections from the domain boundaries need to be considered and the whole process can be approximated as axi-symmetric. The later enables a fast simulation framework calibration.

The specimen used in the present paper is a cube of side length $a = 100\,\text{mm}$ made from the S355J2 steel of density $\rho = 7850\,\text{kg}\,\text{m}^{-3}$, Poisson ratio $\nu = 0.28$, yield strength $\sigma_y = 334\,\text{MPa}$ and chemical composition as listed in Tab 1. The specimen with (not to scale) laser spot is depicted in Fig. 1b.

The cube specimen was prepared utilizing standard machining technologies, which generate non-homogeneous residual stresses in its surface layer. In order to relax these stresses and obtain a stress-free sample, the specimen was subjected to heat treatment. The heat treatment consisted of two times repeated four hours long normalizing at $895\,^{\circ}\text{C}$ and of a stress-relief annealing during which the specimen was heated to $650\,^{\circ}\text{C}$ at the rate of $50\,^{\circ}\text{C}\,\text{h}^{-1}$, kept at $650\,^{\circ}\text{C}$ for three hours, and slowly cooled back to the room temperature at the rate of $50\,^{\circ}\text{C}\,\text{h}^{-1}$.

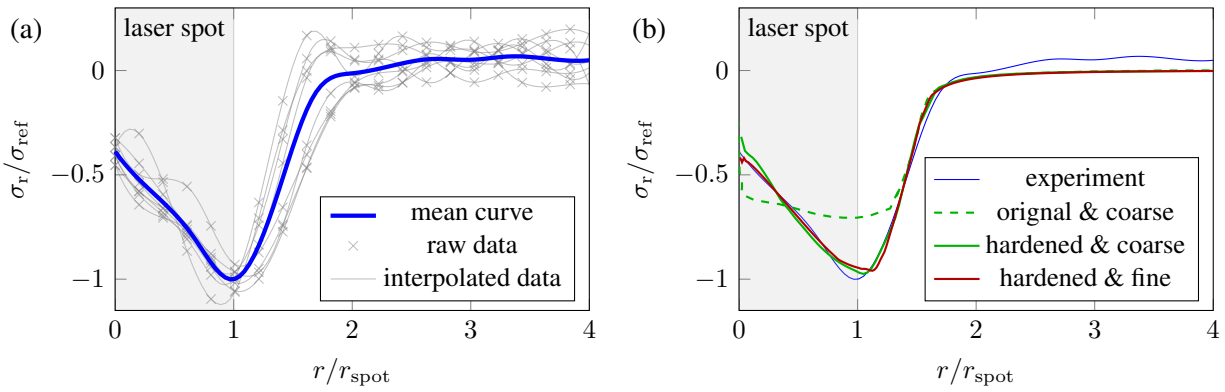

Fig. 2: (a) Measured residual stresses on specimen surface. (b) Model calibration – material pseudo-hardening and mesh resolution independence of results.

Results The framework calibration results are depicted in Fig. 2. In Fig. 2a, we show the available calibration data for a single LSP shot. During postprocessing, the data are interpolated utilising second-order splines that are averaged to obtain the mean curve. Next, the model parameters, $\tilde{p}_0$, $p_{\max}$, $\tilde{r}_{\max}$, T_{t}, and σ_y are adjusted to fit the mean curve as close as possible. For Fig. 2 and all the subsequent plots, $\sigma_{\mathrm{ref}} = 344\,\mathrm{MPa}$ was seleced such that the minimum of the mean curve has the vertical coordinate of -1.

Fig. 2b contains comparison of calibrated model results and mean curve obtained from the experiment. The "original" material has $\sigma_y = 334\,\mathrm{MPa}$, i.e., as provided by the specimen material certificate. The "hardened" material has σ_y as one of the calibrated parameters, which resulted in $\sigma_y = 600\,\mathrm{MPa}$. The "coarse" mesh is a uniform axi-symmetric mesh with 50 finite volume cells per r_{spot}. The "fine" mesh has 100 cells per r_{spot}. Based on the comparison of "fine" and "coarse" mesh results, in the following, we work with the mesh resolution corresponding to the "coarse" mesh.

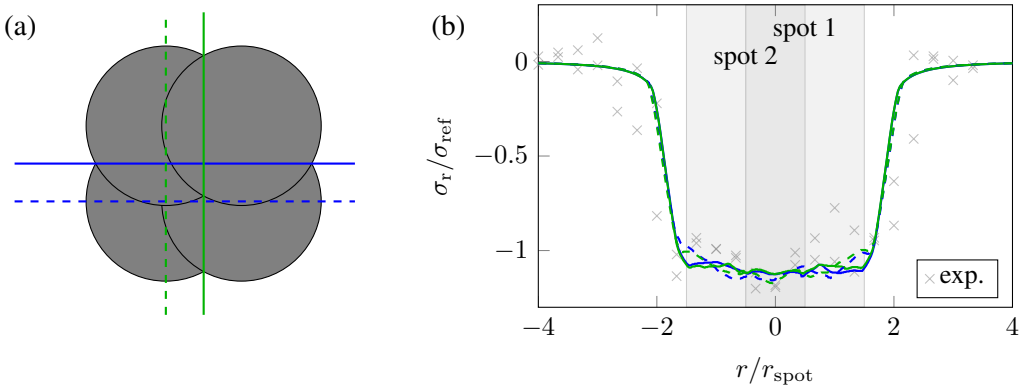

Fig. 3: Model validation. (a) Sampling lines, experiment + simulation (solid), only simulation (dashed). (b) Measured and estimated residual stresses for four overlapping laser spots

After the model calibration on the single-shot experiment, the model is validated on data corresponding to a simple quadruple shot pattern made on the same specimen, see Fig. 1b. The data-sampling lines for the model validation are shown in Fig. 3a. The validation results are given in Fig. 3b. Note the model capability to predict both the treated zone dimensions and the magnitude of the induced residual stresses.

4. Conclusions

We presented a finite-volume method based framework for simulations of laser shock peening. The model was calibrated to estimate residual surface stress generated by a single LSP shot. The model predictive capabilities were successfully validated via prediction of surface residual stresses induced by four partially-overlapping LSP shots. The calibrated framework can be used to simulate laser peening effects on parts made from the same material and processed utilizing the same LSP conditions as was used for its calibration.

Acknowledgments

The work was financially supported by the institutional support RVO:61388998 and by the grant project with No. TM04000048 of the Technology Agency of the Czech Republic.

References

Braisted, W. and Brockman, R. (1999) Finite element simulation of laser shock peening. *International Journal of Fatigue*, 21, pp. 719–724.

Cardiff, P., Tukovic, Z., Jaeger, P. D., Clancy, M., and Ivankovic, A. (2017) A Lagrangian cell-centred finite volume method for metal forming simulation. *International Journal For Numerical Methods In Engineering*, 109, pp. 1777–1803.

Fabbro, R., Fournier, J., Ballard, P., Devaux, D., and Virmont, J. (1989) Physical study of laser-produced plasma in confined geometry. *Journal of Applied Physics*, 68, pp. 775–784.

Hfaiedh, N., Peyre, P., Song, H., Popa, I., Ji, V., and Vignal, V. (2015) Finite element analysis of laser shock peening of 2050-t8 aluminium alloy. *International Journal of Fatigue*, 70, pp. 480–489.

OpenCFD (2007) *OpenFOAM: The Open Source CFD Toolbox. User Guide Version 1.4, OpenCFD Limited*. Reading UK.

Penner, S. S. and Sharma, O. (1966) Interaction of laser radiation with an absorbing semi-infinite solid bar. *Journal of Applied Physics*, 37, pp. 2304–2308.